Mathematical Biosciences and Engineering

http://www.aimspress.com/journal/MBE

MBE, 16(6): 7009–7021.
DOI: 10.3934/mbe.2019352
Received: 24 December 2018
Accepted: 16 July 2019
Published: 01 August 2019

Research article

A fit of CD4$^+$ T cell immune response to an infection by lymphocytic choriomeningitis virus

Atefeh Afsar[1], Filipe Martins[1,*], Bruno M. P. M. Oliveira[2] and Alberto A. Pinto[1]

[1] Departamento de Matemática, Faculdade de Ciências da Universidade do Porto and LIAAD-INESC. Rua do Campo Alegre, 687, 4169-007 Porto, Portugal

[2] Faculdade de Ciências da Nutrição e Alimentação da Universidade do Porto, and LIAAD-INESC. Rua Dr. Roberto Frias, 4200-465 Porto, Portugal

* **Correspondence:** Email: philip_m90@hotmail.com.

Abstract: We fit an immune response model to data reporting the CD4$^+$ T cell numbers from the 28 days following the infection of mice with *lymphocytic choriomeningitis virus* LCMV. We used an ODE model that was previously used to describe qualitatively the behaviour of CD4$^+$ T cells, regulatory T cells (Tregs) and interleukine-2 (IL-2) density. The model considered two clonotypes of T cells in order to fit simultaneously the two time series for the gp61 and NP309 epitopes. We observed the proliferation of T cells and, to a lower extent, Tregs during the immune activation phase following infection and subsequently, during the contraction phase, a smooth transition from faster to slower death rates. The six parameters that were optimized were: the beginning and ending times of the immune response, the growth rate of T cells, their capacity, and the two related with the homeostatic numbers of T cells that respond to each epitope. We showed that the ODE model was able to be calibrated thus providing a quantitative description of the data.

Keywords: T cells; Regulatory T cells (Tregs); *Lymphocytic choriomeningitis virus* (LCMV); epitope gp61; epitope NP309; antigenic stimulation; fit

1. Introduction

T cells are one of the components of the adaptive immune system. They are a subset of lymphocytes that mature in the thymus and are responsible for searching for pathogens. The presence of a pathogen will result in the presentation of its characteristic peptides by the antigen presenting cells (APC) [1]. When T cells of a given clonotype find their specific peptide, they will become activated and they will start secreting cytokines, namely interleukine 2 (IL-2), that signal to other components of the immune system and promote proliferation [2]. However, it may happen that a clonotype of T

cells erroneously target self-antigens, thereby promoting an auto-immune response against its host. Regulatory T cells (Tregs) are a subset of T cells that have immune suppressive function – they are able to inhibit cytokine secretion by T cells [3–8]. At a genetic level, Tregs express Foxp3, a master regulator of the Treg phenotype inducing CD25, CTLA-4 and GITR expression, all correlating with a suppressive phenotype [9]. Auto-immune diseases may appear when Tregs are misregulated, e.g. IPEX [9].

Regarding laboratory data obtained *in vivo* or *in vitro*, there is a large literature on the subject, see, for instance, the reviews by Zhu *et al.* [2, 10]. However, *in vivo* data on time evolution of the concentration of T cells with several measurements over a period of days or months are relatively scarce. One example is the data on immune response by T cells from mice infected with *lymphocytic choriomeningitis virus (LCMV)* by Homann *et al.* [11]. *In vivo* time series can be important to further understand immune response dynamics and to validate existing deterministic or stochastic immune response models.

Modelling of immune responses by T cells can be made using different mathematical tools. See Callard *et al.* [12] and Lythe *et al.* [13] for reviews. De Boer *et al.* [14], Burroughs *et al.* [3], Pinto *et al.* [15], Blyuss *et al.* [16] and Khailaie *et al.* [17] studied systems of ordinary differential equations (ODE), while León *et al.* [18] used a hypergeometric distribution in a discrete model, and Bianca and Brézin [19] used thermostatted kinetic theory methods. In [20] the authors studied bifurcations and employ stochastic modelling with the goal of addressing individual variability as well as variability in the immune system as a whole by means of the Doob-Gillespie algorithm.

In this paper we use the ODE model with two clonotypes in Pinto *et al.* [15], based on the model from Burroughs *et al.* [3]. The model with two clonotypes was previously used to qualitatively describe the appearance of autoimmune diseases after an infection due to the bystanter proliferation of the clonotype of autoimmune T cells [21] and the suppression of autoimmune responses as a consequence of decrease of the clonotype of autoimmune T cells during an infection with sufficiently long duration [22]. Previous analysis of the model with one clonotype [3, 23] showed that T cells' growth due to cytokine has a quorum population threshold as suggested in de Boer *et al.* [14]. For the reported values of the parameters, below a given threshold of antigen stimulation of T cells $b < b_L$, only one stable equilibrium is found - a controlled state with a low concentration of T cells. Above a higher threshold of antigenic stimulation of T cells $b > b_H$, only one stable equilibrium is present - an immune response state, characterized by a high concentration of T cells. Between the two antigenic stimulation thresholds, for b in $[b_L, b_H]$, there is a bi-stability region, where both an immune response state and a controlled state are present. The thresholds b_L and b_H are saddle-node bifurcation points that bound the hysteresis, see e.g. [3, 22]. Moreover, some parameters can unfold the hysteresis at a cusp bifurcation point [23–25]. When a linear tuning between the antigenic stimuli of T cells and Tregs is considered, we observe that the thresholds of antigenic stimulation of T cells can change substantially with the slope parameter and we can also observe a transcritical bifurcation and other saddle-node bifurcations [26, 27]. See also the reviews by Burroughs *et al.* [28] and by Pinto *et al.* [15].

In this paper, we aim to calibrate the ODE model by obtaining a quantitative fit to data, thereby complementing the qualitative description of the properties of the model from previous publications. Thus, we fit the time dynamics of the ODE model to the data from Homann *et al.* [11] regarding the $CD4^+$ T cell numbers responding to LCMV epitopes gp61 or NP309. Previously, de Boer *et al.* [29] fitted the data on the same epitopes considering two or three separate phases. The first phase of their

model is an exponential growth phase, when the immune system is stimulated. It is followed by one or two exponential decay phases, when the stimulation is small. De Boer *et al.* used the same methodology to study data from other epitopes in a different publication [30]. We use a different model from de Boer *et al.* since we consider simultaneously two clonotypes of T cells, Tregs and IL-2; and our ODE system includes non-linear terms. The novelty of our approach is to fit a unique ODE model to the growth and decay phases, where only the antigenic stimulation of T cells may have different values between the immune response phase and the contraction phase. This article is structured as follows. We start by describing the adopted immune response model to fit the data in Section 2. Next, in Section 3 we fit the model to the data. Finally, in Section 4 we present a discussion and an analysis of the results obtained in the fits. The parameters of the model are presented in the Appendix A.

2. Immune response model

We use the model from Section 3 in Pinto *et al.* [15] for $CD4^+$ T cells and regulatory T cells described by a set of ordinary differential equations. We consider one population of Tregs (R, R^*) and two populations of conventional T cells $(T_b, T_b{}^*)$ and $(T_c, T_c{}^*)$, responding to different antigens. Both populations of T cells and Tregs require specific antigenic stimulation for activation. Levels of antigenic stimulation are denoted by a for Tregs and by b and c for conventional T cells. T cells are activated by their specific antigen, from a non-secreting state, denoted T_b or T_c, to a IL-2 secreting state $T_b{}^*$ or $T_c{}^*$. In this paper, the values of b and c can change along time as a consequence of pathogen presence. Similarly, Tregs are activated by self antigens at a constant level a from an inactive state R, to an active state R^*. Tregs do not secrete IL-2. Conventional T cells acquire proliferative capacity in the presence of IL-2. Some authors suggest that Tregs proliferate *in vivo* with IL-2 [4, 5, 8], while the opposite may happen *in vitro* [7]. We will consider that Tregs also proliferate in the presence of IL-2, although less efficiently than normal T cells [3, 15]. Secreting T cells T^* can revert to the non-secreting state T at a rate k or due to the non-specific suppression by active Tregs R^*, at a rate proportional to γ. Nevertheless, non-secreting T cells are still able to proliferate in the presence of IL-2 [6, 9]. Moreover, we consider two types of death terms: linear, the d terms, and quadratic, the β terms. The latter acts as a saturation mechanism and can be related to Fas-FasL death by apoptosis [31, 32]. Finally, we include an influx of (auto) immune T cells into the tissue (T_b^{in} and T_c^{in}) and Tregs (R_{in}), which can represent previously activated T cells from circulation or naïve T cell input from the thymus. This model does not include memory cells explicitly, hence it may only be suited to simulate time evolutions over a few weeks.

The model consists of a set of seven ordinary differential equations. We have a compartment for each T cell population (inactive Tregs R, active Tregs R^*, non-secreting T cells T_b and T_c, and secreting T cells $T_b{}^*$ and $T_c{}^*$) and interleukine 2 density I.

$$\begin{aligned}
\frac{dR}{dt} &= (\epsilon\rho I - \beta N - d_R)R + \hat{k}(R^* - aR) + R^{in},\\
\frac{dR^*}{dt} &= (\epsilon\rho I - \beta N - d_{R^*})R^* - \hat{k}(R^* - aR),\\
\frac{dT_b}{dt} &= (\rho I - \beta N - d_T)T_b + k(T_b{}^* - bT_b + \gamma R^* T_b{}^*) + T_b^{in},
\end{aligned}$$

$$
\begin{aligned}
\frac{dT_b{}^*}{dt} &= (\rho I - \beta N - d_{T^*})T_b{}^* - k(T_b{}^* - bT_b + \gamma R^* T_b{}^*),\\
\frac{dT_c}{dt} &= (\rho I - \beta N - d_T)T_c + k(T_c{}^* - cT_c + \gamma R^* T_c{}^*) + T_c^{in},\\
\frac{dT_c{}^*}{dt} &= (\rho I - \beta N - d_{T^*})T_c{}^* - k(T_c{}^* - cT_c + \gamma R^* T_c{}^*),\\
\frac{dI}{dt} &= \sigma(T_b{}^* + T_c{}^* - (\alpha N + \delta)I),
\end{aligned}
$$

with $N = R + R^* + T_b + T_b{}^* + T_c + T_c{}^*$. The parameters for this model and the ranges considered in the optimization procedure for the fits are given in the appendix (A) in Tables 1 and 2. We will consider the death rates to be equal $d_T = d_R$ and $d_{R^*} = d_{T^*}$. We also assume equal relaxation rates $k = \hat{k}$. Furthermore, we allow for different inflows of T cells T_b^{in} and T_c^{in} and Tregs R^{in}.

3. Simulations and fits

In this section we do the fitting of the immune response model described in the previous section to the data from Homann *et al.* [11]. The data consist of two time series that characterize the immune response by $CD4^+$ T cells to *lymphocytic choriomeningitis virus* - LCMV in mice obtained from laboratory experiments. Each time series corresponds to the total number of T cells that respond to one of the LCMV epitopes studied here: gp61 and NP309.

Most of the parameters of the model were obtained from the literature [3, 15, 23, 33–37] and we assumed those presented in Table 1 to be fixed *a priori*. In Table 2 we list the parameters that were part of the optimization procedure to obtain the fit. These parameters are the T cell maximum growth rate ρ/α, the capacity of T cells T^{cap}, the level of homeostatic T_b cells that are triggered by the gp61 epitope, and the ratio between the homeostatic levels of T cells that are triggered by the NP309 epitope with those triggered by the gp61 epitope.

The pathogen was considered to be present within a limited period of time. To model this we used step functions for the antigen simulation parameters b and c, with specific parameters for each clonotype of T cells responding to each epitope: b_{max} for the gp61 epitope and c_{max} for the NP309 epitope. More precisely, we assumed b and c to be functions of time having a certain high antigen stimulation intensity $b = b_{max}$ and $c = c_{max}$ within a given time interval $t \in [t_{ini}, t_{end}]$, and very small values, $b = 10^{-5}$ and $c = 10^{-5}$ outside that interval.

The values of the six parameters of the fit were obtained from the optimization procedure. The software used for the simulations of the model was GNU Octave - *version 4.2.2* and the routine that was used for the numerical integration of the ODE system was `lsode`. The initial condition of the system (at time $t = 0$) for each set of parameters was obtained by simulating the system for a long time with small values of antigenic stimulations of T cells, $b = c = 10^{-5}$. This allowed us to obtain an initial condition close to the homeostatic controlled state, with a low total number of T cells.

The optimization procedure aimed to minimize the sum of squares of the residuals in a log scale, i.e. to minimize

$$
res^2 = \sum_{i=1}^{14} \left(\log x_b(t_i) - \log(T_b(t_i) + T_b{}^*(t_i))\right)^2 + \sum_{i=1}^{8} \left(\log x_c(t_i) - \log(T_c(t_i) + T_c{}^*(t_i))\right)^2
$$

where the values $x_b(t_i)$ and $x_c(t_i)$ are the observations of total T cell numbers from Homann *et al.* [11] for the gp61 and NP309 epitopes respectively, t_i represents the time of each observation and $T_b(t_i) + T_b{}^*(t_i)$ and $T_c(t_i) + T_c{}^*(t_i)$ the total T cell numbers as obtained from the ODE fit at time t_i. The total residual sum of squares has two components, one corresponding to the gp61 epitope time series res_b^2 and another corresponding to the NP309 epitope time series res_c^2.

The optimum parameter estimates were obtained by using Octave's routine `fminsearch` implementing the Nelder-Mead algorithm/downhill simplex method. We started by running the algorithm on 500 random initial points in the six-dimensional parameter space. Due to numerical accuracy issues, the algorithm could stop at local sup-optimal minimum points. Hence, we had the necessity of running the algorithm repeatedly from distinct initial points. The best fit estimates of the parameters to the data, as well as 95% confidence intervals are presented in Table 2. The confidence intervals were obtained by deviating each parameter from the optimal value until the residual sum of squares was significantly larger - according to the F statistic - than the minimum residual [38]. The fit is presented in Figure 1 together with the residual mean square $MNSQ = res^2/df$, where the number of degrees of freedom df is the difference between the number of data points and the number of free parameters. For epitope gp61 we have that $res_b^2 = 0.565$ and for epitope NP309 we have $res_c^2 = 0.995$. Hence, for $14 + 8 - 6 = 16$ degrees of freedom, we have that $MNSQ = 0.0975$.

We observe in Figure 1 that the total number of T cells responding to either epitope follows the data from Homann *et al.* [11]. Before t_{ini} the system has not detected the presence of a pathogen, thus being in homeostasis. During this period, the numbers of non-secreting T cells T_b and T_c are very close to their respective total. Between t_{ini} and t_{end}, the numbers of secreting T cells $T_b{}^*$ and $T_c{}^*$ initially dominate, and that after day 7, approximately, the numbers of the non-secreting T cells become larger than the numbers of secreting T cells. This happens because the number of Tregs (R and R^*) increases due to the increased presence of IL-2. When the number of active Tregs R^* is sufficiently high, the suppressive action of Tregs is stronger than the antigenic stimulation of T cells. Hence, as the number of active Tregs increases, the secretion of IL-2 cytokines becomes increasingly inhibited, thus reducing the proportion of secreting T cells, even if the total number of T cells is still increasing. Moreover, the overall larger numbers of cells result in an increased Fas-FasL (quadratic) death rate, thereby decreasing the balance between growth and death. After t_{end}, growth halts, since the antigenic stimulation of T cells nearly vanishes. Hence, almost all the secreting T cells relax to their non-secreting state leading to a very low secretion rate of IL-2 and to its quick decay. Therefore, in this phase, the dynamics is governed by the death terms. Initially, the Fas-FasL quadratic death term dominates the contraction phase of all cells. As their number is decreasing, the rate of change is regulated by the balance between the linear death and the inflow of cells into the system.

Besides the fit for the first 4 weeks we also obtained the fit for a time span of 3 weeks (13 data points for epitope gp61 and 7 data points for epitope NP309) and 8 weeks (13 data points for epitope gp61 and 7 data points for epitope NP309). In both cases, the fitted values of the parameters belong to the confidence intervals in Table 2: for the 3 weeks fit we obtained: $MNSQ = 0.0745$, $\rho/\alpha = 2.06$, $T^{cap} = 1.22 \times 10^7$, $T_b^{hom} = 2480$, $T_c^{hom}/T_b^{hom} = 0.279$, $t_{ini} = 3.23$, and $t_{end} = 9.36$; while for the 8 weeks fit we got: $MNSQ = 0.1207$, $\rho/\alpha = 2.15$, $T^{cap} = 2.54 \times 10^7$, $T_b^{hom} = 1732$, $T_c^{hom}/T_b^{hom} = 0.363$, $t_{ini} = 3.22$, and $t_{end} = 8.50$.

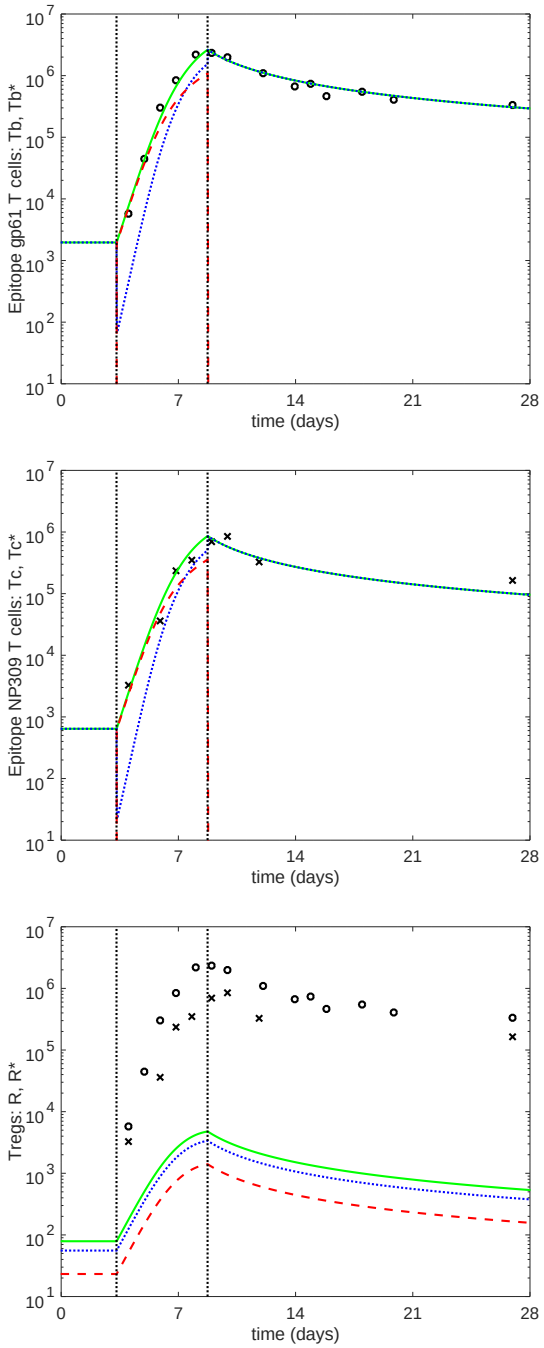

Figure 1. Dynamics for the best fit of the ODE model to the laboratory measurements of CD4$^+$ T cells numbers from Homman *et al.* [11]. $MNS\,Q = 0.0975$. Circles: gp61 epitope data. Crosses: NP309 epitope data. The vertical axis is in logarithmic scale. The vertical dashed lines mark the time of the beginning $t_{ini} = 3.31$ and the end $t_{end} = 8.74$; of the immune response phase. The parameters of the fit are shown in Tables 1 and 2.
Top: Total $T_b + T_b^*$ (green line); non-secreting T_b (blue dots); secreting T_b^* (red dashes).
Middle: Total $T_c + T_c^*$ (green line); non-secreting T_c (blue dots); secreting T_c^* (red dashes).
Bottom: Total $R + R^*$ (green line); inactive R (blue dots); active R^* (red dashes).

4. Discussion

Our simulations can fit the data both in the period of high antigenic stimulation around the first week, and afterwards until day 28, during the contraction phase. De Boer *et al.* [29] analyzed previously the data from Homann *et al.* [11]. Regarding epitope gp61, their model with a biphasic contraction model had a residual mean square $MNSQ_{gp61} = 0.06$, while the one with a single contraction phase had $MNSQ_{gp61} = 0.17$. Regarding the NP309 epitope, their fits had similar residual mean squares: both the biphasic contraction model $MNSQ_{NP309} = 0.10$ and the single contraction model $MNSQ_{NP309} = 0.12$. We note that our model is different since we are fitting simultaneously the data from gp61 and NP309 epitopes using 7 non-linear ordinary differential equations, we use two death terms and we change the antigenic stimulations of T cells b and c in time, instead of having a distinct linear differential equation for each phase, as in de Boer *et al.* [29]. Using step functions for the antigenic stimulation of T cells can be interpreted biologically as the pathogen being either present or not at each time period, which is a simplification of reality in itself. However, when considering the transition from the immune response phase to the contraction phase, using step functions for parameters b and c should not differ substantially from using a distinct equation in each phase, since the transitions between the non-secreting and the secreting states occur in time scales of hours, while data are daily. However, the non-linearities of the model we used, allowed for a smooth fit during the contraction phase.

The assumption of the initial condition being the controlled state is consistent with the assumption that the mice T cells were in a homeostatic state, which is also consistent with the laboratory methodology described in [11] that reports the mice being infected at 6-8 weeks of age. In our fit, a larger homeostatic population of T cells responding to epitope gp61, $T_b^{hom} > T_c^{hom}$, and similar growth rates for both populations of T cells, yields a similar outcome at day 8-9 to the model presented in de Boer *et al.* [29] in which at around day 3, the concentration of T cells is similar for both clonotypes, but the growth rate of the T cells responding to epitope gp61 is larger. We note that in our model, the growth rate of T cells is not constant since it is a function of the concentration of the IL-2 cytokine, which in turn depends on the concentration of secreting T cells. Thus, we were not surprised by finding that the fitted value of the maximum growth rate was higher than the average growth rate reported by de Boer *et al.* [29].

The chosen value of the death rate of T cells is lower than the death rate of the first decay phase, the apoptosis phase, in de Boer *et al.* [29], being closer to the death rate of memory T cells from the second phase. Other small values of the death rate resulted in fits with similar mean square residuals. Thus, we opted to keep the death rate parameter fixed. We note that our model did not consider the differentiation to memory cells which led us to consider only the first 28 days of the data in Homann *et al.* [11]. This may represent a limitation that might be addressed in the future by considering a different model with a specific compartment for memory T cells. The asymmetry in the death rates between secreting and non-secreting T cells, from Pinto *et al.* [15], was present since we considered more than one clonotype of T cells (see also e.g. Burroughs *et al.* [21] and Oliveira *et al.* [22]). As for the fitted values for time spans of 3 weeks and time spans of 8 weeks, we observed that they were within the confidence intervals for the fits for 4 weeks, hence exhibiting no sensitivity at least with respect to small changes in the considered time span. Regarding the Fas-FasL death term, it allows a continuous deceleration of the death rate during the contraction period. We can observe this effect more visibly in Figure 4 (A) of

Pinto *et al.* [15]. This deceleration can be explained by the different relative importance of the death terms along time. After the end of the immune activation phase, while the population size of T cells is still large, the Fas-FasL death rate, proportional to the square of the concentration of T cells, is also high. Hence, we observe an apoptosis phase, characterized by a fast decrease in T cell numbers. As the T cells die, this quadratic term looses relevance and the death rate approaches the linear death term. This smooth behavior is qualitatively similar to the biphasic contraction phase described in de Boer *et al.* [29].

Another limitation is to consider that the antigenic stimulations of T cells b and c, and thus pathogen activation intensity, are step functions of time instead of smooth functions, which might be more realistic. However, this would add more parameters to the model. We recall that the parameters that were kept constant had their values obtained from the literature, and we opted to have the same values for both epitopes due to the small number of data points available. Biologically, having the same values may be interpreted as meaning that the respective characteristics of the T cells are similar for the two epitopes.

We used a model that has processes occurring in different time scales, from minutes, to hours to days. The laboratory restrictions, that led to a small number of data points for a continuous time fit, allow for other models to obtain good fits to the data from Homann *et al.* [11]. Furthermore, to better understand the time dynamics of Tregs in immune responses, we would require that their numbers were also measured. Hence, the homeostatic number of Tregs may be different. Other parameter values had fits with similar residual mean squares, provided the secretion inhibition was adjusted accordingly (data not shown). Nevertheless, in our fit, the presence of Tregs is felt on the decrease of the growth rate, observed at the end of the immune activation phase.

Our model has two main strengths. Firstly, it fits simultaneously the data for the gp61 and NP309 epitopes using the same equations in all phases, the immune activation phase and the contraction phase, and without the need to consider biphasic regimes. Secondly, with respect to the gp61 and NP309 epitopes, only the T cells homeostatic values were different.

For the future, it would be interesting to study human data on the concentration of T cells and Tregs, over large periods of time, ideally measured with a small time resolution. With longitudinal data, we could observe the natural occurrence of infections and the following recovery. This data would allow the researchers to use mathematical tools to create and to validate dynamical models with the inclusion of memory cells, that are key to develop long term immunity to some infections. Moreover, dynamics of auto-immune diseases could also be studied and modelled, and in the process we could estimate parameters and their confidence intervals. However, ethical aspects of such studies should be carefully evaluated, weighting the benefits and the costs.

In conclusion, the model we used allows to be calibrated to obtain a good fit to the data from Homann *et al.* [11] keeping most of the parameters fixed at the values obtained from the literature, and optimizing a set of 6 parameters that are related with the beginning and ending times of the immune response, the maximum growth rate of T cells, the T cells capacity, and the homeostatic numbers of T cells responding to gp61 and NP309 epitopes. Therefore, besides the qualitative features of the model described in other publications, we showed that this model is suited to describe quantitatively immune responses by $CD4^+$ T cells.

Acknowledgements

The authors would like to thank the financial support by the ERDF – European Regional Development Fund through the Operational Programme for Competitiveness and Internationalization – COMPETE 2020 Programme within project "POCI-01-0145-FEDER-006961" and by national Funds through the FCT – Fundação para a Ciência e a Tecnologia (Portuguese Foundation for Science and Technology) as part of project UID/ EEA/ 50014/ 2013, and within project "Dynamics, Optimization and Modelling" with reference PTDC/ MAT-NAN/ 6890/ 2014 as part of project "Modelling, Dynamics and Games" with reference PTDC/MAT-APL/31753/2017 and project "NanoSTIMA – Macro-to-Nano Human Sensing: Towards Integrated Multimodal Health Monitoring and Analytics" with reference NORTE-01-0145-FEDER-000016, financed by the North Portugal Regional Operational Programme (NORTE 2020), under the PORTUGAL 2020 Partnership Agreement. Atefeh Afsar would like to thank the financial support of FCT - Fundação para a Ciência e a Tecnologia - through a PhD. grant of the MAP-PDMA program with reference PD/BD/142886/2018.

Conflict of interest

The authors declare no conflict of interest.

References

1. J. Banchereau, F. Briere, C. Caux, et al., Immunobiology of dendritic cells, *Annu. Rev. Immunol.*, **18** (2000), 767–811.
2. J. Zhu and W. E. Paul, CD4 T cells: fates, functions, and faults, *Blood*, **112** (2008), 1557–1569.
3. N. J. Burroughs, B. M. P. M. Oliveira and A. A. Pinto, Regulatory T cell adjustment of quorum growth thresholds and the control of local immune responses, *J. Theor. Biol.*, **241** (2006), 134–141.
4. A. L. Cava, Tregs are regulated by cytokines: Implications for autoimmunity, *Autoimmun. Rev.*, **8** (2008), 83–87.
5. B.-I. Moon, T. H. Kim and J.-Y. Seoh, Functional modulation of regulatory T cells by IL-2, *PLoS One*, **10** (2015), 1–13.
6. E. M. Shevach, R. S. McHugh, C. A. Piccirillo, et al., Control of T-cell activation by $CD4^+$ $CD25^+$ suppressor T cells, *Immunol. Rev.*, **182** (2001), 58–67.
7. A. M. Thornton and E. M. Shevach, $CD4^+$ $CD25^+$ immunoregulatory T cells suppress polyclonal T cell activation *in vitro* by inhibiting interleukine 2 production, *The Journal of Experimental Medicine*, **188** (1998), 287–296.
8. L. A. Turka and P. T. Walsh, IL-2 signaling and CD4+ CD25+ Foxp3+ regulatory T cells, *Front. Biosci.*, **13** (2008), 1440–1446.
9. S. Sakaguchi, Naturally arising $CD4^+$ regulatory T cells for immunological self-tolerance and negative control of immune responses, *Annu. Rev. Immunol.*, **22** (2004), 531–562.
10. J. Zhu, H. Yamane and W. E. Paul, Differentiation of Effector CD4 T Cell Populations, *Annu. Rev. Immunol.*, **28** (2010), 445–489.

11. D. Homann, L. Teyton and M. B. Oldstone, Differential regulation of antiviral T-cell immunity results in stable CD8+ but declining CD4+ T-cell memory, *Nat. Med.*, **7** (2001), 913–919.
12. R. E. Callard and A. J. Yates, Immunology and mathematics: crossing the divide, *Immunology*, **115** (2005), 21–33.
13. G. Lythe and C. Molina-París, Some deterministic and stochastic mathematical models of naïve T-cell homeostasis, *Immunol. Rev.*, **285** (2018), 206–217.
14. R. J. de Boer and P. Hogeweg, Immunological discrimination between self and non-self by precursor depletion and memory accumulation, *J. Theor. Biol.*, **124** (1987), 343–369.
15. A. Pinto, N. Burroughs, F. Ferreira, et al., Dynamics of immunological models, *Acta Biotheor.*, **58** (2010), 391–404.
16. K. Blyuss and L. Nicholson, The role of tunable activation thresholds in the dynamics of autoimmunity, *J. Theor. Biol.*, **308** (2012), 45–55.
17. S. Khailaie, F. Bahrami, M. Janahmadi, et al., A mathematical model of immune activation with a unified self-nonself concept, *Front. Immunol.*, **4** (2013), 474.
18. K. León, A. Lage, and J. Carneiro, Tolerance and immunity in a mathematical model of T-cell mediated suppression, *J. Theor. Biol.*, **225** (2003), 107–126.
19. C. Bianca and L. Brézin, Modeling the antigen recognition by B-cell and T-cell receptors through thermostatted kinetic theory methods, *Int. J. Biomath.*, **10** (2017), 1750072.
20. R. F. Alvarez, J. A. Barbuto and R. Venegeroles, A nonlinear mathematical model of cell-mediated immune response for tumor phenotypic heterogeneity, *J. Theor. Biol.*, **471** (2019), 42–50.
21. N. Burroughs, M. Ferreira, B. Oliveira, et al., Autoimmunity arising from bystander proliferation of T cells in an immune response model, *Math. Comput. Modell.*, **53** (2011), 1389–1393.
22. B. M. P. M. Oliveira, R. Trinchet, M. V. Otero-Espinar, et al., Modelling the suppression of autoimmunity after pathogen infection, *Math. Methods Appl. Sci.*, **41** (2018), 8565–8570.
23. B. M. P. M. Oliveira, I. P. Figueiredo, N. J. Burroughs, et al., Approximate equilibria for a T cell and Treg model, *Appl. Math. Inform. Sci.*, **9** (2015), 2221–2231.
24. N. Burroughs, B. Oliveira, A. Pinto, et al., Immune response dynamics, *Math. Comput. Modell.*, **53** (2011), 1410–1419.
25. N. Burroughs, B. Oliveira, A. Pinto, et al., Sensibility of the quorum growth thresholds controlling local immune responses, *Math. Comput. Modell.*, **47** (2008), 714–725.
26. N. Burroughs, M. Ferreira, B. Oliveira, et al., A transcritical bifurcation in an immune response model, *J. Differ. Eq. Appl.*, **17** (2011), 1101–1106.
27. B. M. P. M. Oliveira, A. Yusuf, I. P. Figueiredo, et al., The effect of a linear tuning between the antigenic stimulations of T cells and Tregs. In Preparation.
28. N. J. Burroughs, M. Ferreira, J. Martins, et al., Dynamics and biological thresholds, in *Dynamics, Games and Science I, DYNA 2008, in Honor of Maurício Peixoto and David Rand* (editors A. A. Pinto, D. A. Rand, and M. M. Peixoto), volume 1 of *Springer Proceedings in Mathematics*, Springer-Verlag Berlin Heidelberg (2011), pp. 183–191.

29. R. J. de Boer, D. Homann and A. S. Perelson, Different Dynamics of CD4+ and CD8+ T Cell Responses During and After Acute Lymphocytic Choriomeningitis Virus Infection, *J. Immunol.*, **171** (2003), 3928–3935.

30. R. J. de Boer and A. S. Perelson, Quantifying T lymphocyte turnover, *J. Theor. Biol.*, **327** (2013), 45–87.

31. R. E. Callard, J. Stark and A. J. Yates, Fratricide: a mechanism for T memory-cell homeostasis, *Trends Immunol.*, **24** (2003), 370–375.

32. S. Nagata, Fas ligand-induced apoptosis, *Annu. Rev. Genet.*, **33** (1999), 29–55.

33. P. M. Anderson and M. A. Sorenson, Effects of route and formulation on clinical pharmacokinetics of interleukine-2, *Clin. Pharmacokinet.*, **27** (1994), 19–31.

34. A. R. Mclean and C. A. Michie, In vivo estimates of division and death rates of human t lymphocytes., *Proceedings of the National Academy of Sciences*, **92** (1995), 3707–3711.

35. C. Michie, A. McLean, C. Alcock, et al., Life-span of human lymphocyte subsets defined by CD45 isoforms, *Nature*, **360** (1992), 264–265.

36. D. Moskophidis, M. Battegay, M. Vandenbroek, et al., Role of virus and host variables in virus persistence or immunopathological disease caused by a non-cytolytic virus, *J. Gen. Virol.*, **76** (1995), 381–391.

37. H. Veiga-Fernandes, U. Walter, C. Bourgeois, et al., Response of naïve and memory $CD8^+$ T cells to antigen stimulation *in vivo*, *Nat. Immunol.*, **1** (2000), 47–53.

38. G. A. Seber and C. J. Wild, *Nonlinear Regression*, Wiley and Sons (2003).

A. Appendix

The parameters of our model and their default values are presented in the following two tables.

Table 1. Fixed parameter values for the model of T cells and Tregs from [3, 15, 23, 33–37]. The formula for the maximum cytokine concentration is obtained from [3, 23].

Fixed Parameters	Symbol	Value
T cells T_b, T_b^*, T_c, T_c^*		
Death rate of inactive T cells (day^{-1})	d_T	10^{-3}
Death rate ratio of active : inactive T cells	d_{T^*}/d_T	0.1
Secretion reversion[2] (day^{-1})	k	2.4
Maximum antigen stimulation level of T_b cells	b_{max}	100
Maximum antigen stimulation level of T_c cells	c_{max}	100
Tregs R, R^*		
Growth rate ratio Tregs : T cells	ϵ	0.6
Relaxation rate (day^{-1})	$\hat{k}$	2.4
Death rate ratio of inactive Tregs : inactive T cells	d_R/d_T	1
Death rate relative ratio of Tregs : T cells	$\frac{d_{R^*}}{d_R}/\frac{d_{T^*}}{d_T}$	1
Tregs antigen stimulation level (day^{-1})	$a\hat{k}$	1
Homeostatic Treg level[3] (cells day^{-1})	R^{hom}	100
Secretion inhibition	γ	$10/R^{hom}$
Interleukin-2 (IL-2) Cytokine		
Max. cytokine concentration[4] (pM)	$1/\alpha$	200
IL2 secretion rate (pM day^{-1})	σ	144
Cytokine decay rate (day^{-1})	$\sigma\delta$	36

[1] Maximum T cell density for severe infections (based on LCMV).

[2] This is in the absence of Tregs.

[3] Tregs input level is given by $R^{in} = R^{hom}\left(d_R - \frac{\hat{k}a(d_R - d_{R^*})}{d_{R^*} + \hat{k}(1+a)}\right)$.

[4] This is taken as 20 times the receptor affinity ($10pM$).

Table 2. Fitted parameter values and 95% confidence intervals for the model of T cells and Tregs. $MNSQ = 0.0975$. The formulas for the T cell maximum growth rate and the capacity of T cells were obtained from [3, 23].

Parameter	Symbol	Fitted value	95% CI[1]
T cell maximum growth rate (day^{-1})	ρ/α	2.06	[1.82, 2.35]
Capacity of T cells[1] (10^7 cells)	$T^{cap} = \rho/(\alpha\beta)$	1.76	[1.10, 2.99]
Homeostatic T_b cells level[2] (cells day^{-1})	T_b^{hom}	2409	[1637, 3677]
Homeostatic levels ratio[3] $T_c^{hom} : T_b^{hom}$	T_c^{hom}/T_b^{hom}	0.327	[0.204, 0.527]
Beginning of the immune activation phase (day)	t_{ini}	3.31	[3.00, 3.59]
End of the immune activation phase (day)	t_{end}	8.74	[7.94, 9.91]

[1] 95% confidence interval.
[2] T_b cell input level is given by $T_b^{in} = T_b^{hom} d_T$.
[3] T_c cell input level is given by $T_c^{in} = T_b^{in}\, T_c^{hom}/T_b^{hom}$.